

Simulations of the Interaction Region in a Photon-Photon Collider

P. Chen^a, T. Ohgaki^b, A. Spitkovsky^c, T. Takahashi^{b1} and K. Yokoya^d

^aStanford Linear Accelerator, Stanford University, Stanford, CA94309, USA

^bDepartment of Physics, Hiroshima university, Higashi-Hiroshima, 739, Japan

^cDepartment of Physics, University of California at Berkeley, Berkeley, CA 94720, USA

^dKEK-National Laboratory for High Energy Physics, 1-1 Oho, Tsukuba, 305, Japan

Abstract

The status and initial performance of a simulation program CAIN for interaction region of linear colliders is described. The program is developed to be applicable for e^+e^- , e^-e^- , $e^-\gamma$ and $\gamma\gamma$ linear colliders. As an example of an application, simulation of a $\gamma\gamma$ collider option of NLC is reported.

1 Introduction

As additional options of e^+e^- linear colliders, feasibility studies for e^-e^- , $e^-\gamma$ and $\gamma\gamma$ colliders have become active in recent years. For linear colliders, detailed knowledge of beam-beam interaction is important to estimate backgrounds in the detector as well as to calculate realistic luminosity. In order to study these effects, a Monte Carlo simulation program for beam-beam interaction in e^+e^- colliders, ABEL (Analysis of Beam-beam Effects in Linear colliders), was developed [1]. The original ABEL included beam disruption and beamstrahlung [2] and was later modified (ABELMOD) [3] to include electron-positron pair creation which is potentially a serious source of background to the detector [4].

For e^-e^- , $e^-\gamma$ and $\gamma\gamma$ colliders, a similar kind of simulation is necessary to understand beam-beam interaction, but the situation is much more complicated due to the necessarily complex schemes of the beam collision. In $e^-\gamma$ and $\gamma\gamma$ colliders, an intense laser beam is flashed on the incoming electron beam just before the interaction point to convert high energy electron beam to high energy photon beam by Compton scattering [5]. A simulation program for these colliders is required to implement laser-electron interaction at the conversion point which is typically on the order of cm upstream from the interaction point. In addition to the conversion point, the simulation of beam-beam interaction at the interaction point is more complicated than in the e^+e^- collider case, since 1) the initial state includes not only electrons and positron but also photons, 2) as a consequence of Compton interaction at the conversion point, electron and photon beams have wider

¹corresponding author. e-mail address: tohrut@kekux1.kek.jp

spectrum in both energy and spatial distribution than those of e^+e^- colliders. According to these features, it is necessary to develop a new simulation program for beam-beam interaction. To meet this requirement, a project to write a new comprehensive beam-beam simulation program named CAIN (Conglomerat d'ABEL et d'Interactions Non-lineares) [4] was launched with the intention to include Compton and Breit-Wheeler processes at conversion point, transport of particles from conversion point to interaction point and interaction of all possible combinations of electrons/positrons and photons at the interaction point. By using the Compton scattering part of CAIN, the effect of Breit-Wheeler process in a photon-photon collider is discussed in previous paper[5].

In this paper, we report the first version of the comprehensive simulation program which can treat conversion, transportation and interaction region in a single framework and is applicable for handling of all 4 types of e^+e^- , e^-e^- , $e^-\gamma$ and $\gamma\gamma$ colliders. As examples of the simulation, differential luminosity distribution of $\gamma\gamma$, e^-e^- and e^+e^- option of NLC is described.

2 Structure of CAIN (version 1.0)

A schematic of a $\gamma\gamma$ collider is illustrated in fig.1. An intense laser pulse is flashed on the electron beam at the conversion point (CP) where high energy photon beams are produced by Compton scattering. Photons and electrons coming out from CP are transported for O(cm) to the interaction point (IP). At the transport region (TP), spent electrons from CP may be swept out by an external magnetic field or possibly plasma lens to avoid the electron collision at the IP. Electrons and photons that are transported to the IP collide with positrons and photons from another beam.

Corresponding to the scheme of the $\gamma\gamma$ collider, simulations in CAIN are divided in three modules CP, TP and IP as illustrated in fig.2. In this figure, particles and processes included in each step are shown as well.

At the CP, Compton and Breit-Wheeler interactions between laser and electron beams are simulated. First of all, an electron bunch is divided into given number of macro particles and initial position and momentum of each macro particle are calculated from beam twiss parameters. In a typical linear collider, the number of electrons per bunch is $O(10^{10})$.

A typical simulation uses 10,000 macro particles, with each one representing $O(10^6)$ electrons. The transverse and longitudinal coordinates in the simulation space are subdivided into cells and macro particles are assigned to these cells according to their position.

The time in the simulation is also divided into steps. In each time step, the probability of Compton scattering is calculated for each macro particle according to the laser intensity, and a Compton scattered photon is generated according to the probability. The local laser intensity at each cell is calculated from given laser parameters by taking into account diffraction effect, i.e.,

$$\sigma_r^L(z) = \sigma_0^L \sqrt{1 + \left(\frac{z}{Z_R}\right)^2}$$

where σ_0^L and $\sigma_r^L(z)$ are RMS spot sizes at the focal point and at distance z from the

focal point of the laser. Z_R is the Rayleigh length of the laser which is defined as;

$$Z_R = \frac{4\pi(\sigma_0^L)^2}{\lambda_L}$$

where λ_L is wave length of the laser. If the Compton scattering event is generated, the new photon is created and momentum of the scattered electron is modified. Such an electron can still interact with the laser in the following time steps.

As is described later, the primary consideration in selecting the laser parameters is keeping the effect of nonlinear QED processes to a minimum. However, it is impossible to avoid such effects completely when high luminosity is required. The nonlinear Compton processes can be expressed as

$$e + n\gamma(laser) \rightarrow e + \gamma$$

where $n\gamma(laser)$ indicates that more than one laser photons are absorbed coherently by a single electron. Since this process accounts for higher tails in scattered photon spectrum and lowers peak energy of photon spectrum due to the increase of effective electron mass [6], it has to be kept small to get good photon beams. For the purpose of $\gamma\gamma$ and $e^-\gamma$ collider application, proper treatment of helicity of electron and laser beam is essential since produced photon energy spectrum depends on the helicity state of incoming electrons and photons. In the simulation, cross section formula by Tsai [7] is used in which the polarization of electrons and laser is taken into account in nonlinear QED calculation. The nonlinear Breit-Wheeler process can be written as

$$\gamma(Compton) + n\gamma(laser) \rightarrow e^+e^-$$

where more than one laser photons are absorbed by (Compton scattered) high energy photon and generate electron positron pairs. This process produces electron-positron pairs even if the center of mass energy of $\gamma(Compton)\gamma(laser)$ system is lower than e^+e^- threshold and could be an additional source of backgrounds in high laser field environment. We also adopt the formula by Tsai [7] for this process.

The transport process takes care of drift of spent electrons, Compton photons and electron positron pairs that come out from CP. Photons are simply drifted to IP according to their angular divergence. For electrons and positrons, however, it is possible to insert a sweeping magnet to deflect them from IP. In the version 1.0 of CAIN, a sweeping magnet and synchrotron radiation in the sweeping process is included by a classical radiation treatment. Since the strength of the sweeping magnetic field is on the order of 1 Tesla, the critical energy of synchrotron radiation is low enough to be treated as the classical radiation. Synchrotron radiation photons are added to the total photon population to be inputted to the interaction region.

IP phenomena are simulated in the same way as done in ABELMOD [1, 3]. In fact, a reworked version of ABELMOD serves as an interaction region module in CAIN 1.0 to simulate disruption of electron beams, generation of beamstrahlung, and production of low energy pairs. The difference from ABELMOD is that CAIN needs to take care of mixture of electrons/positrons and photons as its initial state, while only electron and positron beams could be used in ABELMOD. Thus ABELMOD was modified to treat externally

Table 1: Parameters for a photon-photon collider

Electron beam parameters	
Beam energy	$\mathcal{E}_b=250\text{GeV}$
Number of Particles per bunch	$N = 0.65 \times 10^{10}$
Repetition rate	$f_{rep} = 180\text{Hz}$
Number of bunches per pulse	$n_b = 90$
Bunch length	$\sigma_z=100\mu\text{m}$
Bunch sizes (C.P.)	$\sigma_x=718\text{nm}$
	$\sigma_y=91\text{nm}$
Bunch sizes (I.P.)	$\sigma_x=71\text{nm}$
	$\sigma_y=9.1\text{nm}$
Beta functions (I.P.)	$\beta_x=0.5\text{mm}$
	$\beta_y=0.5\text{mm}$
Emittances	$\gamma\epsilon_x=5.0 \times 10^{-6} \text{ m}\cdot\text{rad}$
	$\gamma\epsilon_y=8.0 \times 10^{-8} \text{ m}\cdot\text{rad}$
CP-IP distance	$b=5\text{mm}$
Laser parameters	
Wave length	$\lambda_L = 1.17\mu\text{m}$
Pulse energy	1 J
Pulse length	$\sigma_z^L = 0.23\text{mm}$
Peak power density	$1 \times 10^{18} \text{ W}/\text{cm}^2$
Repetition rate	same as the electron beam
r.m.s spot size	$\sigma_r^L = 2.9\mu\text{m}$

supplied photons and internally generated beamstrahlung photons on equal footing. In every time step in the interaction region CAIN collects total and differential luminosities of e^+e^- or e^-e^- as well as $\gamma\gamma$ and $e\gamma$ luminosities that are available for graphical display after the simulation.

3 Case Study: $\gamma\gamma$, e^-e^- Collisions in NLC

3.1 $\gamma\gamma$ Collisions

Simulations of $\gamma\gamma$ collisions were performed with the reference parameters for a $\gamma\gamma$ collider option of NLC [9] summarized in Table 1.

With these parameters, geometric luminosity of electron-electron collision is $8.7 \times 10^{33} \text{cm}^{-2} \text{s}^{-2}$ which is larger than the typical NLC e^+e^- collider ($4.3 \times 10^{33} \text{cm}^{-2} \text{s}^{-2}$). Since the luminosity of photon-photon colliders is approximately proportional to the geometric luminosity and, unlike e^+e^- collider, there is no strong beamstrahlung at the interaction, the higher geometric luminosity is preferable. Laser parameters are chosen so that conversion efficiency of incoming electrons in a laser pulse is about 0.65. The peak

laser power density is about $10^{18}W/cm^2$ which corresponds to nonlinear QED parameter

$$\xi^2 = \left(\frac{eE}{\omega mc} \right)^2 \approx 0.4 \left[\frac{I}{10^{18}W/cm^2} \right] \left[\frac{\lambda_L}{1.054\mu m} \right]^2 \approx 0.4$$

where e, E, ω, m, c, I and λ_L are electric charge, strength of laser field, laser photon energy, electron mass, speed of light, laser intensity and laser wave length respectively. Here we assumed that the laser profile has a 3-dimensional Gaussian shape and it can be focused to diffraction limit.

With this set of electron and laser parameters, the Compton kinematic parameter is $x = 4\mathcal{E}_b\omega/m_e^2 = 4.47$ and the maximum photon energy \mathcal{E}_{max} in linear Compton limit is

$$\mathcal{E}_{max} = \frac{x}{x+1}\mathcal{E}_b \approx 200GeV.$$

which is about 80% of the original beam energy.

The treatment of spent electrons coming out from the CP is one of the important issues to be considered in $\gamma\gamma$ colliders. If these electrons collide with electrons and photons from the other beam, beam-beam interaction at the IP generates low energy electron positron pairs. These pairs are a possible source of detector background as in e^+e^- colliders [8]. In this situation, luminosity of $e^-\gamma$ and e^-e^- collision is comparable to $\gamma\gamma$ luminosity which could make physics analysis complicated. For this reason, it is desirable to install magnet between CP and IP to sweep spent electrons away from IP. However, the strength of the magnetic field is needed to be on the order of 1 Tesla for effective deflection of electrons and it is necessary to install the magnet in the very limited space (1cm) between CP and IP.

In addition, the magnet must not interfere with precise measurement of vertex position of, for example, b quark decay. To meet these, much research and development effort is necessary.

Using NLC simulation parameters, we consider two cases of interaction region geometry – without the sweeping magnet between CP and IP, and with it.

Without the magnet, electron beams are collided with $1\sigma_y$ offset so as to reduce electron beam collision without significantly deteriorating $\gamma\gamma$ luminosity.

The energy spectra of Compton scattered photons are plotted in fig.3 for linear and nonlinear QED calculations. In the simulation, it is assumed that the laser beam is 100% circularly polarized and the electron beam is 100% longitudinally polarized. The combination of polarization of laser (P_γ) and electron (P_e) beams is chosen so that $P_\gamma P_e = -1$, which produces a relatively narrow peak at high energy edge. Comparing nonlinear and linear Compton spectra, the maximum energy of photons in nonlinear processes exceeds $\mathcal{E}_{max} = x\mathcal{E}_b/(x+1) \approx 200GeV$ due to multiple laser photon absorption. It is also seen that the high energy peak of about 200GeV in linear Compton is shifted to a lower value in nonlinear spectrum. This is another effect of nonlinear interaction, i.e., increasing of effective electron mass. The peak energy is consistent with the expected value,

$$\mathcal{E}_{max} = \frac{x\mathcal{E}_b}{x + \xi^2 + 1} \approx 190GeV.$$

Table 2: Summary of the luminosity

Linear Compton Simulation	
$L_{\gamma\gamma}$	$0.98L_{geom}$ $0.10L_{geom} \ (z = W_{\gamma\gamma}/2\mathcal{E}_b > 0.65)$
$L_{e\gamma}$	$0.71L_{geom}$ $0.16L_{geom} \ (z > 0.65)$
L_{ee}	$0.10L_{geom}$ $0.05L_{geom} \ (z > 0.65)$
Nonlinear Compton Simulation	
$L_{\gamma\gamma}$	$0.88L_{geom}$ $0.08L_{geom} \ (z > 0.65)$
$L_{e\gamma}$	$0.71L_{geom}$ $0.16L_{geom} \ (z > 0.65)$
L_{ee}	$0.11L_{geom}$ $0.06L_{geom} \ (z > 0.65)$

The differential luminosity spectrum is shown in fig.4 for linear and nonlinear Compton calculations. In $L_{\gamma\gamma}$ distribution, high c.m.s energy contriubution is made by collision of Compton photons. In the low energy region, a large low energy tail is seen in the spectrum. The source of the tail is beamstrahlung, i.e., collisions of beamstrahlung photons with beamstrahlung and Compton photons. With nonlinear calculation, high energy peak is shifted to a lower value due to the shift in Compton photon spectrum, and the peak becomes broader than the linear Compton case. $\gamma\gamma$ luminosity in high energy region is about 8% of geometric luminosity and 10% in linear Compton calculation because of the broadness of the high energy peak. The nonlinear effect lowers the peak energy and broadens the peak; however, with this set of parameters $\xi^2 = 0.4$ and the effect is not very significant and is at tolerable level. Obtained luminosities are summarized in Table 2.

Since there is an overlap of electron beams and of electron and photon beams at the interaction point, some amount of $L_{e\gamma}$ and L_{ee} is observed. From the experimental point of view, the initial state of the interaction should be as simple as possible but should provide high luminosities at the same time. These requirements are conflicting and additional studies are needed to find an optimum solution.

The luminosity distribution for the case with sweeping magnet is shown in fig.5. The simulation parameters of the electron and the laser beams are the same as in the case without the sweeping magnet except for the distance between CP and IP: taking into account comlications of installation of the magnet, CP is shifted to 10mm from the IP. The strength of magnetic field is 1 Tesla in x direction and 250GeV electron is swept 60nm($\approx 6\sigma_y$) away in y direction from IP. As seen in fig.5, $e^-\gamma$ and e^-e^- luminosities are significantly reduced. Comparing with the non-sweeping magnet case, $\gamma\gamma$ luminosity is expected to be reduced due to the enlargement of CP-IP distance while it gains a little bit due to the absense of σ_y offset. As a result, $\gamma\gamma$ luminosity is 6% of geomrtric luminosiry

Table 3: Parameters for a e^+e^- and e^-e^- collider

Electron beam parameters	
Beam energy	$\mathcal{E}_b=250\text{GeV}$
Number of Particles per bunch	$N = 0.65 \times 10^{10}$
Repetition rate	$f_{rep} = 180\text{Hz}$
Number of bunches per pulse	$n_b = 90$
Bunch length	$\sigma_z=100\mu\text{m}$
Bunch sizes (I.P.)	$\sigma_x=286\text{nm}$
	$\sigma_y=4.5\text{nm}$
	$\beta_x=8.4\text{mm}$
Beta functions (I.P.)	$\beta_y=0.126\text{mm}$
Emittances	$\gamma\epsilon_x=5.0 \times 10^{-6} \text{ m}\cdot\text{rad}$
	$\gamma\epsilon_y=8.0 \times 10^{-8} \text{ m}\cdot\text{rad}$

for $z > 0.65$ which is slightly smaller than non-sweeping case(8%).

3.2 Other applications

As the second case study, we applied the program to e^+e^- and e^-e^- collisions in NLC configuration listed in Table 3 with center-of-mass energy $\sqrt{S} = 500\text{GeV}$ [9].

The calculated luminosity is shown in fig.6. The total e^+e^- and e^-e^- luminosity is $1.42L_{geom}$ and $0.55L_{geom}$ respectively. As expected, the e^+e^- luminosity is enhanced by the collective Coulomb interaction (pinch effect) while the e^-e^- luminosity is reduced to almost half of geometric luminosity due to repulsive coulomb interaction at the IP.

To simulate $e^-\gamma$ collider, the laser pulse should be aimed at one electron beam and the other beam should be kept untouched. This simulation is easily set up by the combination of $\gamma\gamma$ and e^-e^- parameters and the results are similar to $\gamma\gamma$ collider without the sweeping magnet.

4 The Next Step: CAIN 2

4.1 Problem in CAIN1.0

As was demonstrated in the previous section, CAIN1.0 can be successfully used for the simulations of general linear collider schemes, however there are some problems with the structure of the program. The main problem comes from the fact that IP simulation of CAIN1.0 is essentially the same as ABEL which was developed for pure e^+e^- simulation.

The IP simulation in CAIN1.0 assumes that each bunch in the initial state consists of a single kind of particle – electron or positron with possible mixture of photons. (For example, the same distribution is used for particle distribution to calculate luminosity and for charge distribution to calculate the beam field.) Although electron positron pairs are created in CP by Breit-Wheeler process, the information on the pair particle species is

ignored in the IP simulation. For most of $\gamma\gamma$ collider parameters, Breit-Wheeler process in CP is kept small and neglecting pair species does not affect the simulation significantly. However, in the case of high laser intensity or high x , large number of electron positron pairs are created at CP and their contribution should not be ignored in the IP simulation.

It is implicitly assumed in CAIN1.0 that the initial energies of electrons/positrons are more or less in the same energy range. However, in the case of $\gamma\gamma$ colliders the energy just before IP has a wide spread from the full energy down to a few percent. This fact makes the various formulas (for example the integration of equation of motion) adopted in CAIN1.0 somewhat inaccurate. In this respect the incoherent pair particles, whose energy can be much lower, have no problem because they are treated in a different way. However, in fact the spent electrons and the incoherent pair particles form an energy spectrum almost continuous from a few MeV to hundreds of GeV. In this sense there is no reason to treat the incoherent pair particles on a different footing.

The orbit angles of incoherent pair particles can be as large as hundred milliradians. Nevertheless, CAIN1.0 assumes that the z -component of the velocity is equal to the velocity of light. This fact makes the orbit calculation somewhat unreliable but it is very hard to modify this point in the framework of CAIN1.0.

There is another problem which is common for both CP and IP simulations. As mentioned, the simulation is performed by macro particles each of which represents, typically, $O(10^6)$ real particles. If one is interested in the effect of smaller number of particles, say, $O(10^3)$, a very large number of macro particles is needed for such a run. This drastically affects program speed and required storage. There are several ways to avoid this, however. One can populate certain regions of the beam (the halo, for instance) with macro particles with reduced weight, thus enhancing resolution only in the regions of interest. Also, the analysis of “light-weight” macro particle behavior can be done after the collective fields have been calculated, thus neglecting the contribution of these particles to the field. These methods are not implemented in CAIN1.0.

4.2 CAIN2 Project

In order to overcome the problems stated above, the simulation program CAIN2 has been written from scratch because the code and memory structure of ABELMOD were not adequate for further extension. The major differences of the structure of the new version CAIN2 are

- All the particles (electron/positron/photon, initial or secondary, etc) are stored in the same array and treated on equal basis. (Laser beams are not treated as particles: they are ‘external fields’ like the field of magnets.)
- Instead of invoking separate programs, various interactions such as laser-Compton, beam-beam interaction and beam transport are processed one by one at every time step in one program, if their flags are on. This will enable to add new interactions, such as plasma, which may take place simultaneously with other interactions.
- The new user interface allows much more variety of the configurations of the beams and interactions so that applications other than linear colliders may be possible.

For example, one can prepare a neutral beam of mixed e^+e^- , a bunch consisting of many bunchlets, etc.

The basic assumption in CAIN1.0 is that the collision of the two beams is collinear, meaning that the crossing angle is very small and that each of the two beams, right-going and left-going, is a well-defined beam, i.e., the mutual angles between the constituents are reasonably small. Without this assumption the calculation of the beam-beam force would be very complex.

This requirement has also been adopted in CAIN2 but it is relaxed in two respects. Firstly, small samples of particles (such that their contribution to the beam field is negligible) can have large angles. This is relevant for incoherent pair particles. Secondly, the right-going and left-going beams can make large angles so long as each beam is well collimated. CAIN2 introduces Lorentz transformation to make the collision collinear. Thus, a large crossing angle can be correctly treated.

The latest version of CAIN2, which is to be completed soon, includes the following interactions:

1. Beam deformation by classical field (mainly the beam field)
2. Quantum-theoretical synchrotron radiation (beamstrahlung)
3. Coherent pair creation (this was missing in CAIN1.0)
4. Linear interaction of lasers with e^- , e^+ , γ .
5. Nonlinear interaction of lasers with e^- , e^+ , γ .
6. Particle-particle interactions such as the incoherent pair creation and bremsstrahlung.

Now, all the processes in CP, TP, and IP can be treated by one program. They can be done in a single job or partitioned into separate jobs.

Since the polarization is very important in various applications, it is included in most of the above interactions. For example, (1) in the above list includes precession in magnetic fields, (2), (3), (4) include all possible polarizations, and (5) includes longitudinal polarization of all the particles, initial and final.

In order to overcome the statistical problem of rare events, most interactions now have the ‘event enhancement factor’. For some interactions it is also possible to enhance the rate of some part of the spectrum so that, for example, one can create more low-energy macro particles (with less weight).

5 Summary

We developed a simulation program for phenomena in the interaction regions of linear colliders which allow us to estimate realistic luminosity distributions and detector backgrounds. This simulation program can be used for various types of linear colliders such as $\gamma\gamma$, $e^-\gamma$, e^-e^- , and e^+e^- by just switching input parameter.

This program was used for a photon-photon collider option of the NLC and a realistic luminosity distribution was obtained. It was also found that nonlinear QED effect is not negligible in typical parameters for a $\gamma\gamma$ collider. Since particle physics issues as well as

amounts of background events depend on the luminosity distribution, it gives us useful information for further study.

Acknowledgments

We would like to thank Profs. K.J. Kim, M. Ronan and Dr. M. Xie of LBL for useful discussions. Two of the authors (T.T. and T.O.) thank Prof. I. Endo for his encouragement.

References

- [1] K. Yokoya, KEK-Report 85-9 (1985); Nucle. Instr. and Meth. **A251** (1986) 1
- [2] P. Chen and V.I. Telnov, Phys. Rev. Lett. **63** (1989) 1796.
- [3] T. Tauchi, K. Yokoya and P. Chen, Part. Acc. **41** (1993) 29.
- [4] P. Chen et. al., Nucl. Instr. Meth.**A335** (1995) 107.
- [5] T. Ohgaki and T. Takahashi, Nucle. Instr. Meth. **A373** (1996) 185
- [6] D.M. Volkov, Z. Phys. **94** (1935) 250
- [7] Y.S. Tsai Phys. Rev. D**48**(1993) 96
- [8] JLC-I KEK-Report 92-16 (1992)
- [9] Zeroth-Order Design Report for the Next Linear Collider, appendix B. SLAC-474

Figure Captions

Fig.1 A Schematic view of a photon linear collider.

Fig.2 The scheme of the simulation. The processes and particles considered in each step is also shown.

Fig.3 Simulated photon energy spectrum from Compton conversion point without (a) and with(b) nonlinear QED effect.

Fig.4 Simulated luminosity distribution of a $\gamma\gamma$ collider without (a) and with (b) nonlinear QED effect. Solid, dashed and dots line corresponds to $\gamma\gamma$, $e^-\gamma$ and e^-e^- luminosity respectively.

Fig.5 Simulated luminosity distribution of a $\gamma\gamma$ collider with sweeping magnet. Solid, dashed and dots line corresponds to $\gamma\gamma$, $e^-\gamma$ and e^-e^- luminosity respectively.

Fig.6 Simulated luminosity distribution of a e^+e^- (a) and e^-e^- (b) collider with NLC parameter.

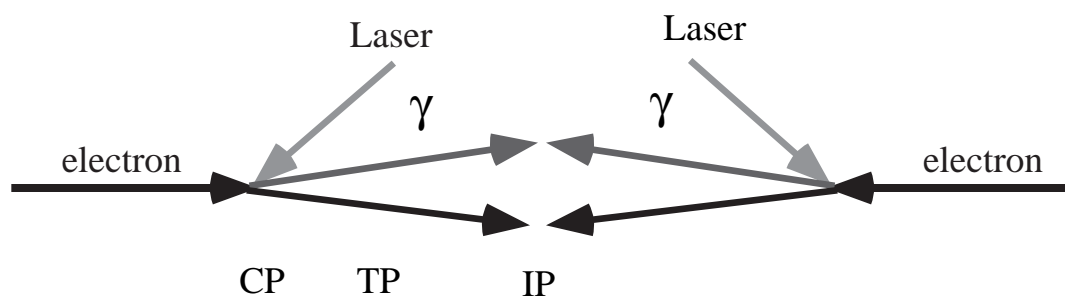


Fig. 1

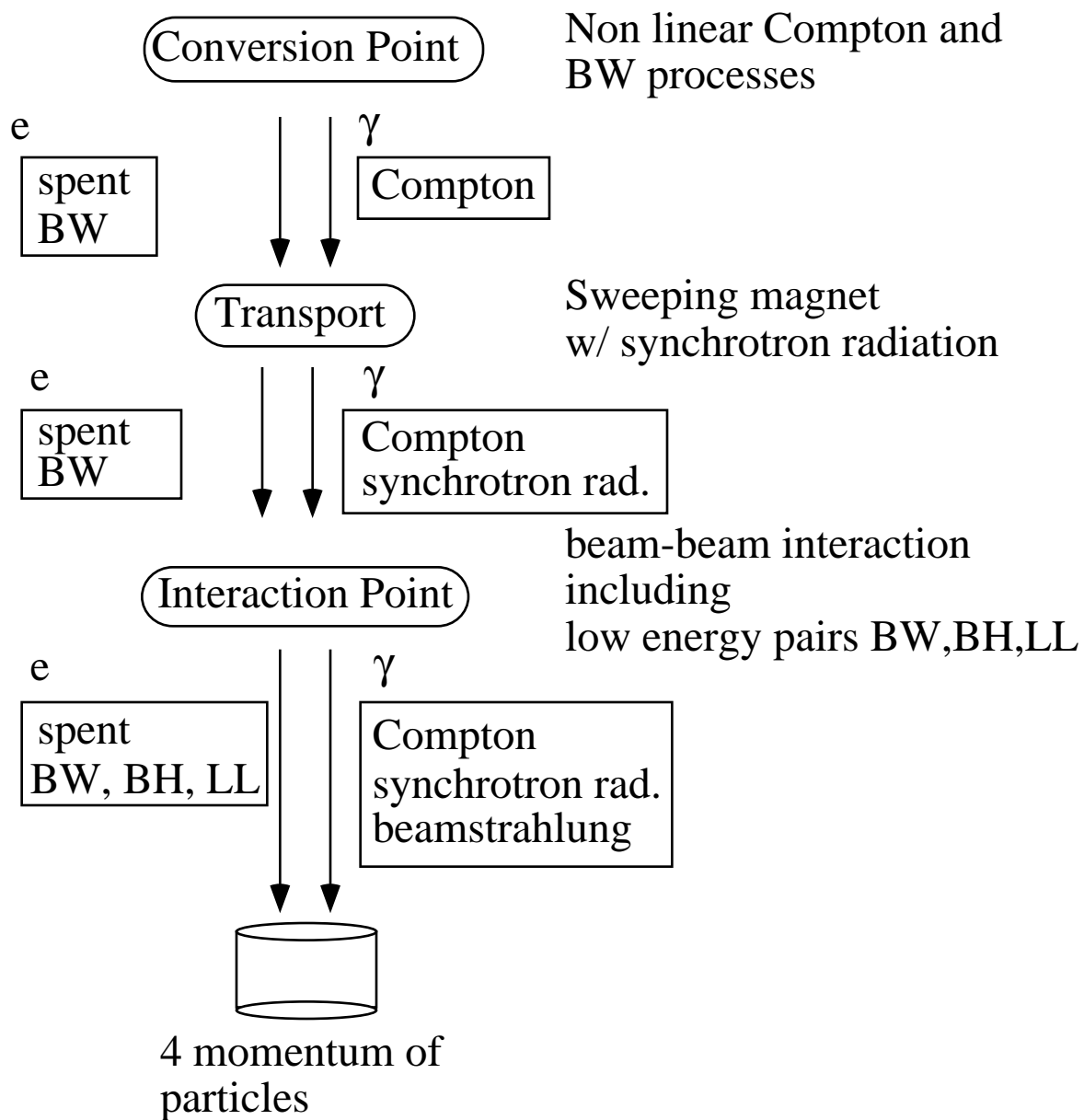


Fig. 2

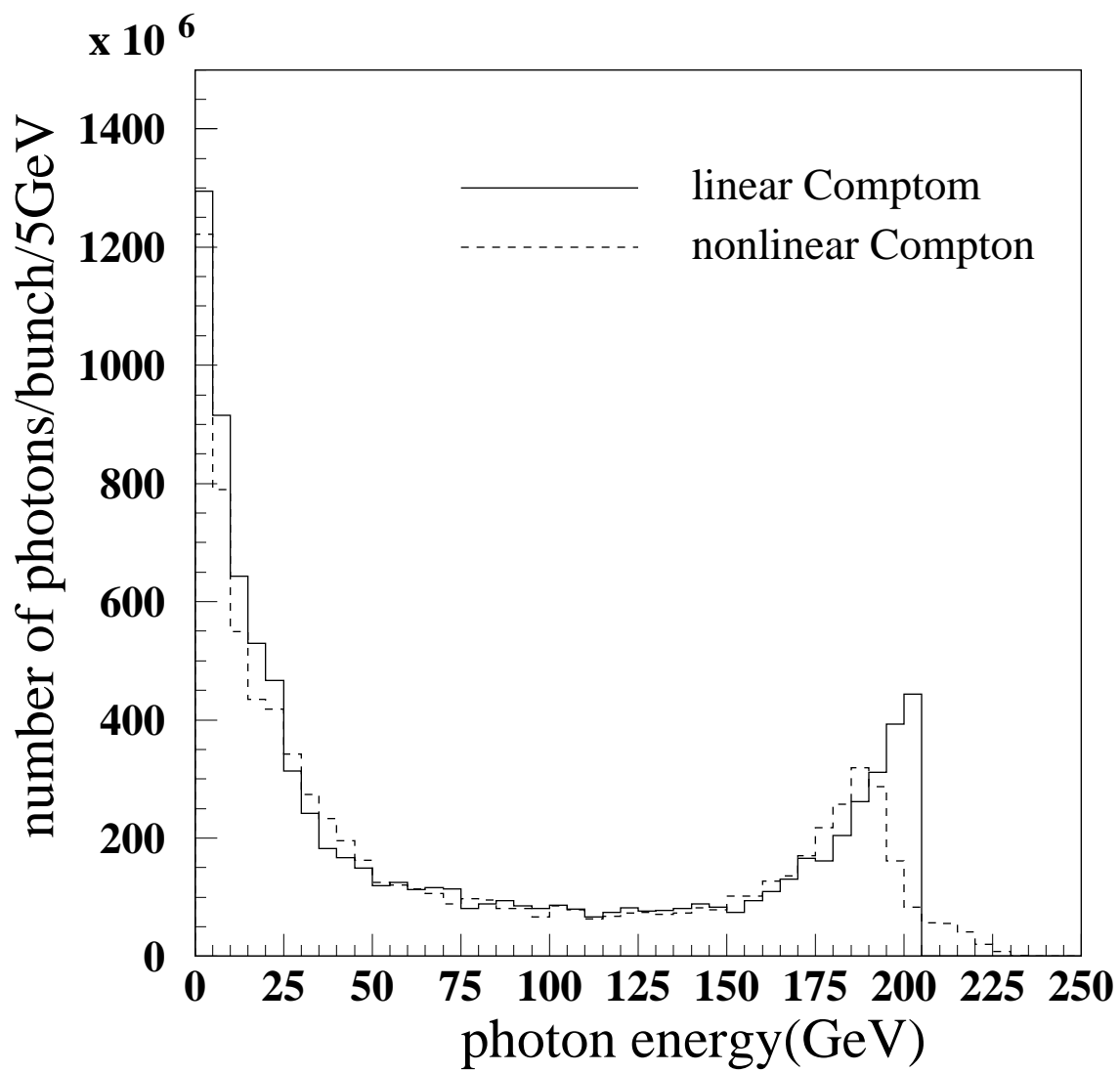


Fig.3

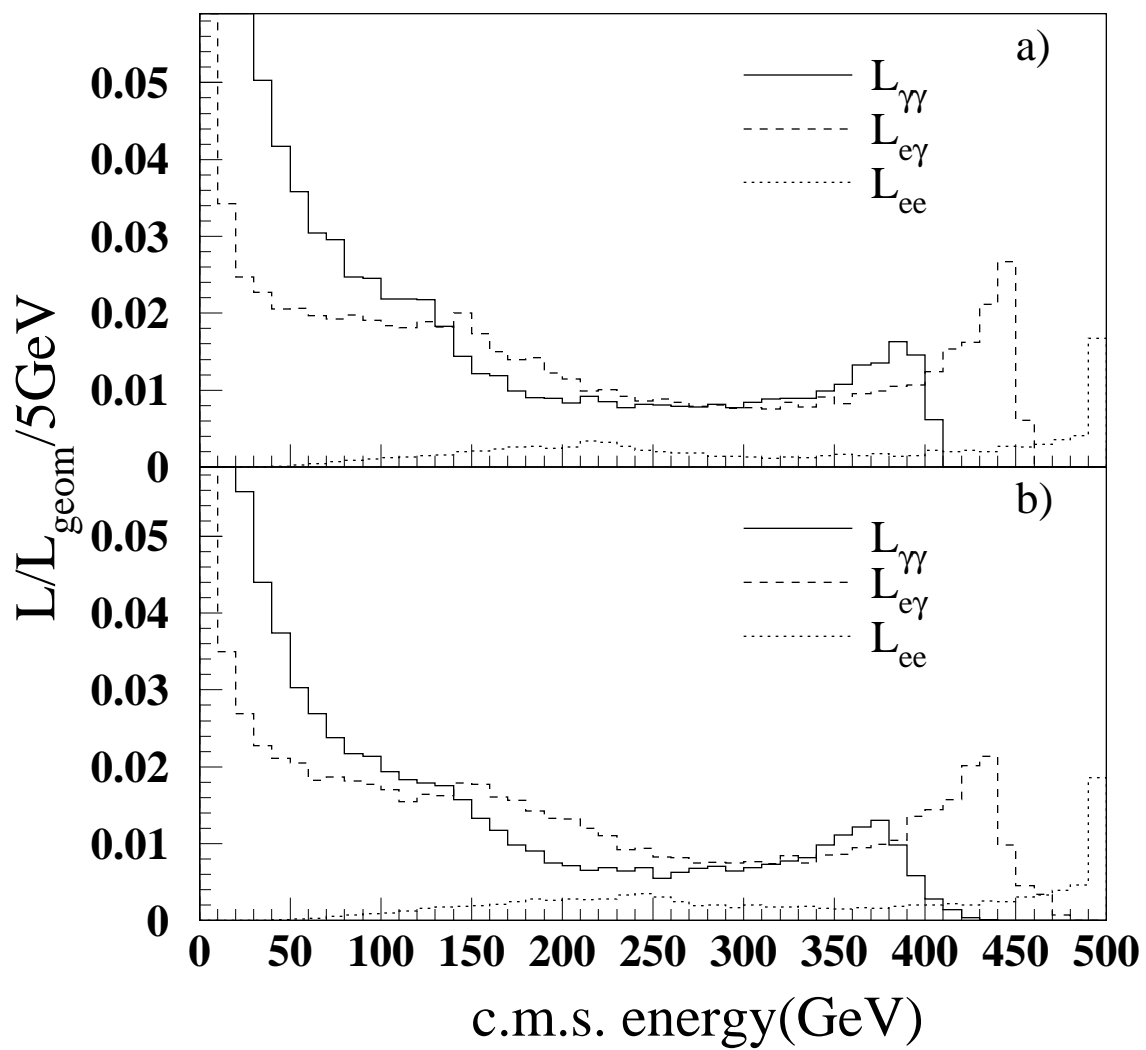


Fig.4

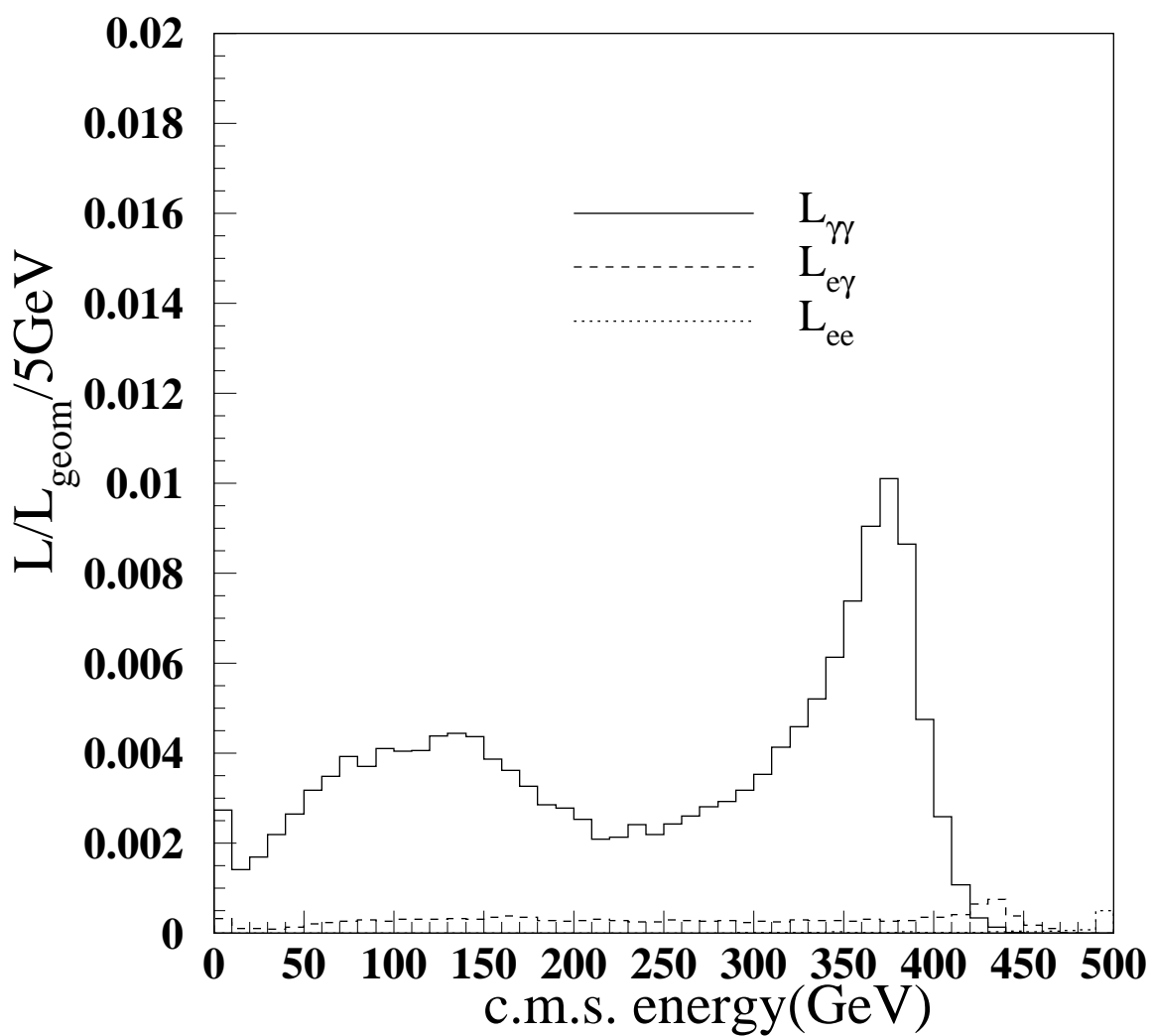


Fig.5

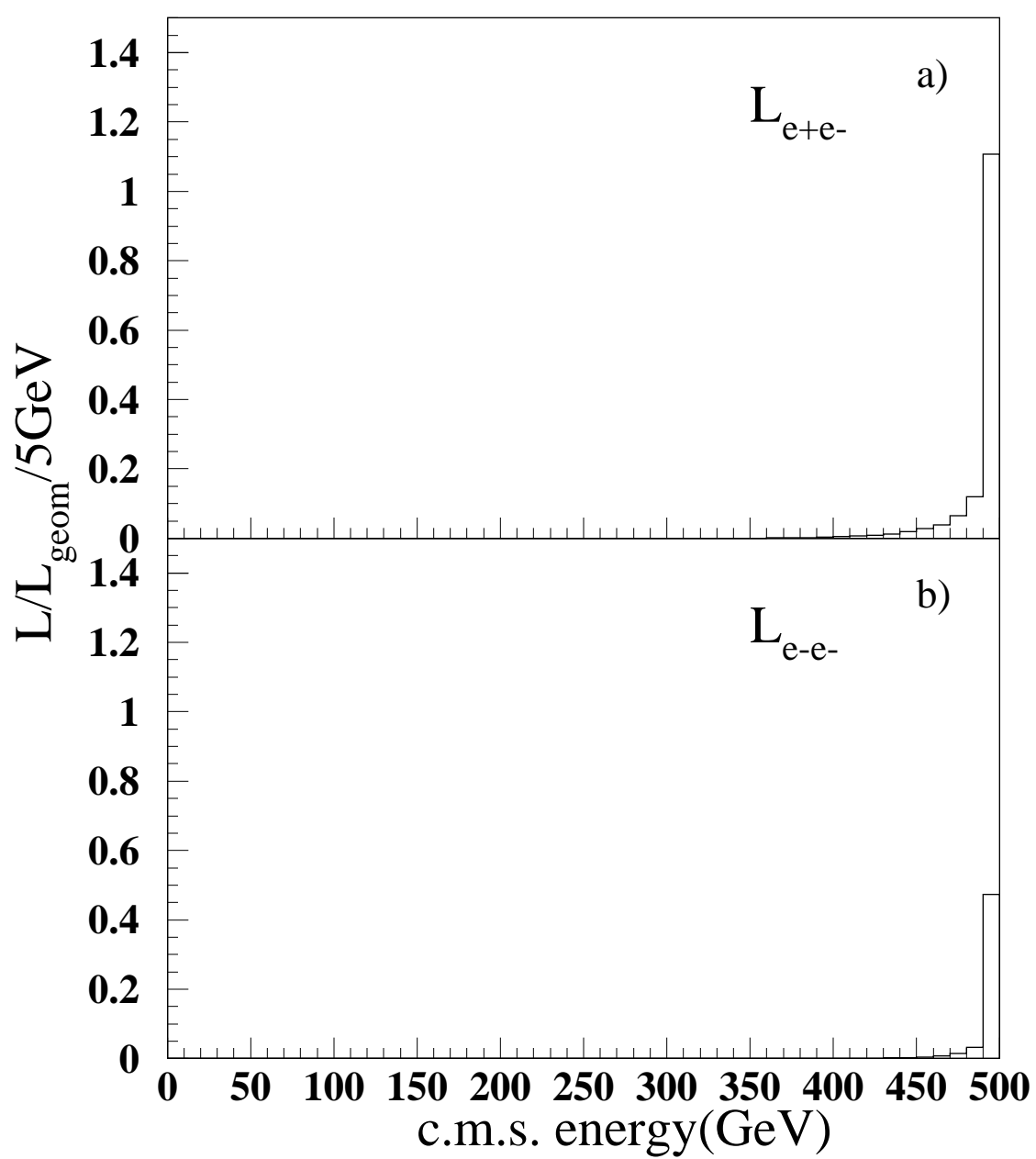


Fig.6